Electrical breakdown in the microscale: Testing the standard theory

Emmanouel Hourdakis,[a] Garnett W. Bryant, and Neil M. Zimmerman
National Institute of Standards and Technology, Gaithersburg, Maryland 20899

(Received 26 May 2006; accepted 25 September 2006; published online 28 December 2006)

We present breakdown voltage measurement data in air taken with a technique we have recently developed and present calculations that show that the common assumption that one protrusion is responsible for the observed current is not warranted. The data suggest that below 10 μm of electrode separation the dominant effect is field emission of electrons. Analyzing the data in that regime, using the theory of standard field emission and field amplification on the surface of a conductor, we come to a prediction about the geometry of the surface protrusions on the electrodes. We look for these protrusions using an atomic force microscope. We find several reasons why the standard theory does not appear to explain our data and conclude that the standard theory is not sufficient. © *2006 American Institute of Physics*. [DOI: 10.1063/1.2400103]

I. INTRODUCTION

Electrical breakdown in a high voltage experiment or electric circuit can cause unwanted currents to flow through a device, degrading its performance or even completely destroying it.[1] In recent years, electronic circuits have become denser, and applications such as microelectromechanicalsystems (MEMSs) use electrodes that are closely separated.[2] An understanding of how breakdown occurs in this regime of micron to submicron separations is thus important in reducing the risks of device failures.

Research in breakdown voltage in air was traditionally done for large separations (order of centimeters) where Paschen's law is relevant.[1] Paschen's law determines the value of the breakdown voltage of air as a function of electrode separation and gas pressure.[3] It is based on the fact that when an electric field exists between two conductors, electrons and ions in the gas will be accelerated. When the positive ions collide with the electrode surfaces, they will force electrons to be emitted. These electrons are, in turn, accelerated by the field and when the field is large enough they ionize air particles through collisions. An avalanche effect is thus created that leads to breakdown.

When the separation between the electrodes is decreased to a length scale comparable to the mean free path of an electron in air (~500 nm), Paschen's law no longer applies. Experiments that have been done in such regime show that the value of the breakdown voltage decreases almost linearly for separations where Paschen's law predicts a fast increase.[4,5] In fact, in this regime breakdown values versus separation are very similar to breakdown curves for vacuum.[6–8] Thus, the process for air breakdown is most likely the same as in vacuum breakdown, which is field emission of electrons from the metallic electrodes. In typical experiments, the value of electric field at which the field emission is observed is as much as a factor of 100 smaller than the value predicted by theory. That discrepancy is thought to be the result of local field amplification on the surface of the electrodes, due to roughness. In most published work in the field, researchers assume the existence of features on the surface of the electrodes that would explain the observed results. There are also a number of studies[9–15] that make surface roughness measurements of the electrodes, but none that actually relate the predictions of the theory to the experimental observables.

In our experiment we measure breakdown voltage in air for separations between 400 nm and 45 μm. We focus on the range below 10 μm where we expect that field emission of electrons is the dominant effect. It is in this range that we observe large deviations from Paschen's curve and the data can be fitted by the field emission theory. We use the standard theory to predict the geometry of protrusions due to surface roughness that would enhance the electric field on the surface. No previous experimental verification of the shape and size of these protrusions exists. We use atomic force microscopy (AFM) measurements to try to locate such surface features. From our results we can show that there are three different reasons for coming to the conclusion that the field amplification theory does not apply in our experiment.

II. FIELD EMISSION OF ELECTRONS

In this section, we present the theory framework that underpins the standard understanding of breakdown at low separations between two planar surfaces.

Electrons in a metal see a surface potential barrier due to the material's work function ϕ. When a field exists, this barrier is deformed. For strong enough fields there is a finite probability of electrons tunneling through it. This is called field emission of electrons.[16,17]

For field emission the current density (J) as a function of the applied electric field (E) is given by the Fowler-Nordheim equation[17]

$$J = DE^2 \exp\left(\frac{-B\varphi^{3/2}}{E}\right), \tag{1}$$

where

[a]Electronic mail: emmanouel.hourdakis@nist.gov

 © 2006 American Institute of Physics

Downloaded 29 Dec 2006 to 129.6.64.224. Redistribution subject to AIP license or copyright, see http://jap.aip.org/jap/copyright.jsp

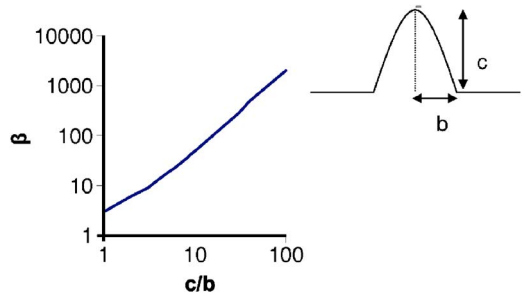

FIG. 1. (Color online) Graph of the dependence of the field amplification factor β on the height to base ratio of a hemispheroid protrusion of height c and base length b.

$$D = \frac{e^3}{16\pi^2\hbar\varphi t^2(y)}, \quad B = \frac{4}{3e}\left(\frac{2m}{\hbar^2}\right)^{1/2} \upsilon(y),$$

from Ref. 18,

$$\upsilon(y) = 0.956 - 1.062y^2,$$

$$t(y) = 1.044,$$

$$y = 3.79 \times 10^{-4}(E^{1/2}/\varphi),$$

and ϕ is the work function of the metal.

Equation (1) shows that for current densities of 10^2–10^3 A/cm^2, which are typical in breakdown experiments, the electric field has to be 3–6×10^7 V/cm.

From experimental results of breakdown in vacuum[6–8] (where the breakdown mechanism is field emission of electrons) the value of the field required to cause breakdown is significantly lower (in some cases by more than a factor of 100) than the value predicted by the Fowler-Nordheim equation. In order to explain this phenomenon, a microscopic enhancement β of the local electric field is introduced. This enhancement is thought to be the result of the existence of protrusions on the surface of the metal. The value of the electric field will be

$$E = \beta\frac{V}{d}, \tag{2}$$

where d is the distance between the metallic surfaces between which V is applied. If we write $J=I/A$, where I is the current and A is the area of the protrusion, we can rewrite Eq. (1) as

$$\frac{I}{V^2} = D\frac{A\beta^2}{d^2}\exp\left(\frac{-B\varphi^{3/2}d}{\beta V}\right). \tag{3}$$

Plotting $\ln(I/V^2)$ vs $1/V$ is the common way of determining the value of β, assuming the value of ϕ is known. The slope of such a plot will be, from Eq. (3),

$$\text{slope} = \frac{-B\varphi^{3/2}d}{\beta}, \tag{4}$$

and the y intercept is

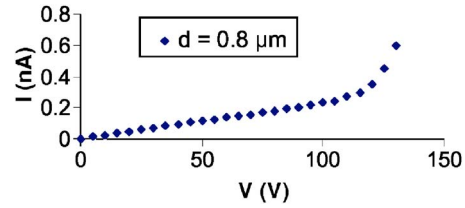

FIG. 2. (Color online) Current vs applied voltage through the capacitor used for breakdown measurements. The data are for 0.8 μm of separation between the plates. V_{break} was chosen as 120 V.

$$y_{\text{int}} = \frac{DA\beta^2}{d^2}. \tag{5}$$

The local field enhancement factor β depends on the geometry of the protrusions on the metallic surface. A protrusion will cause the electric field to concentrate at its tip in an effort to be perpendicular to the metallic surface. Solving Maxwell equations for a hemispheroid protrusion (Fig. 1) and imposing the correct surface boundary conditions (for a dc applied field),[19] the field amplification factor β as a function of the height to base ratio (c/b) is shown in Fig. 1 (note that for $c/b\sim20$, $\beta\sim100$, which would allow for previous interpretations of experimental data[4]).

III. BREAKDOWN RESULTS

We use the method we have recently developed to acquire the values of breakdown voltage for different values of electrode separation. The separation range is from 400 nm to 45 μm. The material used for the electrodes is thermally deposited thin films of Au, for which ϕ=5 eV. The measurement consists of monitoring the current through the air gap capacitor (area of plates is 80×80 μm^2) as the applied voltage is increased. The value of the breakdown voltage is chosen to be where the current starts increasing nonlinearly (Fig. 2). The experimental procedure is described in detail in Ref. 20.

The data acquired with this method are shown in Fig. 3. For separations larger than 10 μm, the data approach Paschen's curve (Paschen's curve is drawn for reasonable values of its parameters). Below 10 μm the main cause of breakdown must be field emission of electrons since this is the only other possibility considering that the separation of the

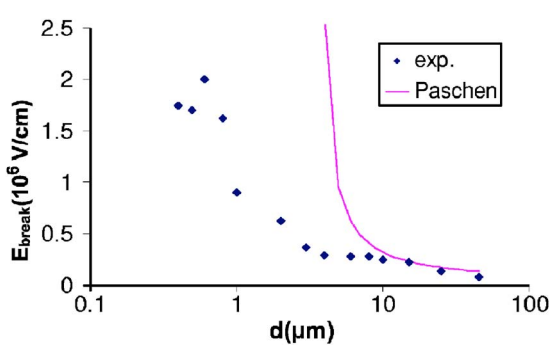

FIG. 3. (Color online) Breakdown electric field as a function of electrode separation (d). The points are experimental results. The red curve represents Paschen's law. Note that, as is standard in the field, E is 25–30 times smaller than 5×10^7 V/cm.

Downloaded 29 Dec 2006 to 129.6.64.224. Redistribution subject to AIP license or copyright, see http://jap.aip.org/jap/copyright.jsp

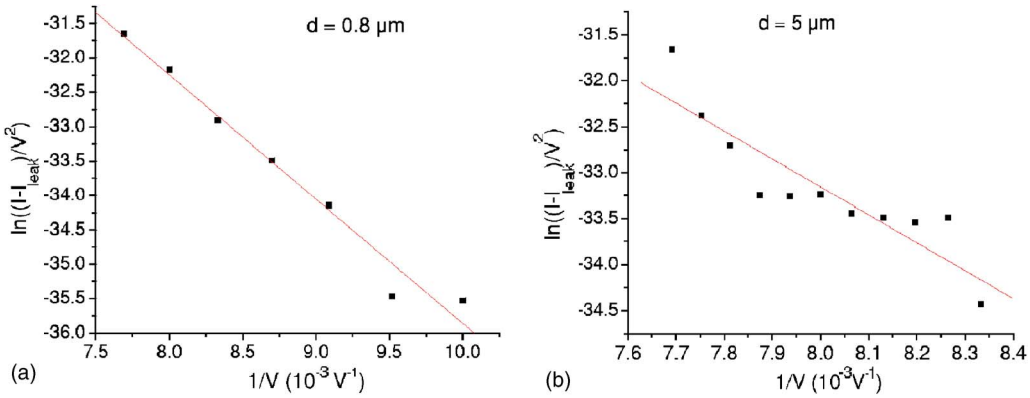

FIG. 4. (Color online) $\ln[(I-I_{\text{leak}}/V^2)(V_0^2/I_0)]$ vs $1/V$ for (a) 0.8 μm of separation and (b) 5 μm of separation. The red line is a linear fit with slope for (a) −1800 V and for (b) −3000 V.

electrodes is large enough to assume that direct tunneling is negligible. This curve is typical of the field. Much of the work in the literature stops here, assuming surface roughness and β factors that would explain the experimental data ($\beta \sim 100$). In what follows we aim to explicitly test these assumptions.

In order to predict what ranges of β factors would satisfy the requirements of the observed current as well as the breakdown voltages, we plot $\ln[(I-I_{\text{leak}}/V^2)(V_0^2/I_0)]$ as a function of $1/V$ [Eq. (3)], where $I_0=1$ nA, $V_0=1$ V, and $I_{\text{leak}}=V/R$ allows subtraction of the linear portion in Fig. 2, which is leakage.

We then fit to get the value of the slope [two examples of this are shown in Figs. 4(a) and 4(b)]. The fact that we can fit the data using the Fowler-Nordheim equation suggests that the cause for breakdown in this regime is in fact field emission. This is the standard argument in the literature. Using Eq. (4) we get a value of β for each data point. Error bars represent the uncertainties in Fig. 5(a). The big value of uncertainty in the calculation of β factors is the result of the fact that we are making a large extrapolation in Fig. 4 to $1/V=0$.

We then use the value of β to calculate the area A of the protrusion responsible for the observed current. We can do that by using the measured values of I and V and Eq. (3). The results of those calculations appear in Fig. 5(b). We note that some values of A (for $d=7$ and 10 μm) are unphysical; they are larger than the area of the electrodes. This is our first piece of evidence that the theory does not explain our data.

IV. SURFACE ROUGHNESS RESULTS

Up to this point, we have followed the standard analysis in the literature of the experimental data. After the calculation of β and the area of the responsible feature, it is generally assumed in this field that such a feature in fact exists on the surface of the electrodes. The fact that we end up with unphysical calculated values of A suggests that further analysis is in order. Thus, we use the theory in order to get predictions of the actual sizes of the features thought to be responsible for the field amplification on the surface of our electrodes. In contrast to previous studies,[5,6,8] we then try to locate features of specific size, using an AFM. We can then directly compare the predictions of the theory with an experimental observable.

Knowing the values of β and the corresponding area of the protrusion, from the analysis in the previous section, we can use Fig. 1 to calculate the height of the protrusion, c, as a function of its base dimension, b. We are assuming $A=b^2$. We report this in Table I, for values of area A, and so b, that are physically possible. We have excluded the data for $d=7$ and 10 μm because for these cases the theory predicts unreasonable values of A [Fig. 5(b)].

We have used the theory to predict the sizes of the protrusions necessary to explain our data. We use an AFM to look at the surface roughness of our metallic electrodes and to try to locate the protrusions with the predicted geometry. For this part an AFM with a 20 nm radius tip was used, in tapping mode. The AFM pictures were taken on samples

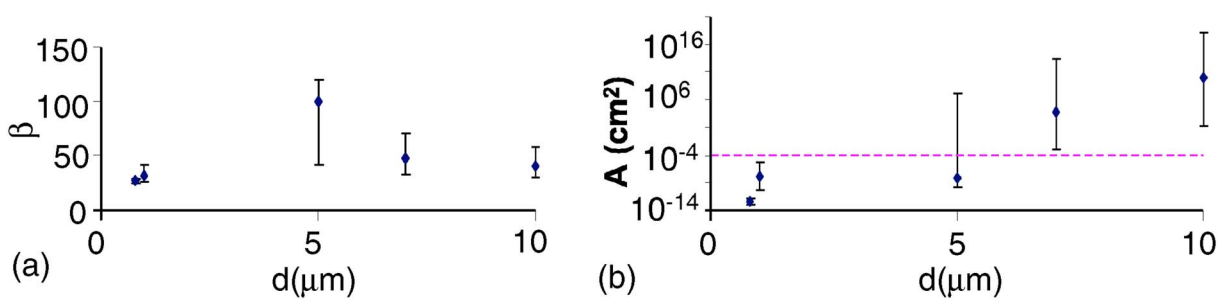

FIG. 5. (Color online) (a) β as a function of electrode separation; (b) emitting area as a function of electrode separation. In both cases the fitting uncertainties are represented with error bars. In (b), the horizontal line represents the maximum area given the device geometry. Note that the two sets are unphysical. This is our first piece of evidence against the theory.

Downloaded 29 Dec 2006 to 129.6.64.224. Redistribution subject to AIP license or copyright, see http://jap.aip.org/jap/copyright.jsp

TABLE I. Calculated minimum and maximum dimensions of protrusions necessary for observed currents at different electrode separations.

d (μm)	0.8		1		5	
	Min.	Max.	Min.	Max.	Min.	Max.
Base (nm)	1.1	20	65	22 000	120	50×10^{12}
Height (nm)	7.7	140	455	154 000	1320	50×10^{13}

before the actual breakdown measurements were taken. This is because all breakdown measurements are done with a new pair of electrodes.[20] The results presented here (Figs. 6 and 7) are typical. In order to check reproducibility, we looked at the electrodes after breakdown measurements using a scanning electron microscope (SEM). The electrodes are smooth, with no visible imperfections, except in discrete regions of size $\sim(100\ \mu\text{m})^2$. In those areas, the large current has caused part of the thin film electrode to vaporize. Since these vaporized regions are not coincident with the capacitor overlap regions where we measured the breakdown, we can conclude that the capacitor electrode surfaces were not altered during the measurement.

Initially we take scans of a large area as in Fig. 6. We then concentrate on areas where there are no visible protrusions (area inside dotted rectangle in Fig. 6). For this area, similar to almost all of the samples' total area, we see that the average roughness is 6 nm. The maximum deviation between low and high points for such areas is $R_{\max}=69$ nm. If protrusions exist in this area their height is not larger than 69 nm.

We then check visible protrusions individually. Three examples are given in Fig. 7. We have done line scans over what seemed to be protrusions of large height. As is clear from Fig. 7, the height to base ratio is much smaller than what is required by the theory. Table I gives the minimum and maximum base and height dimensions for the predictions of the theory not excluded by the value of A.

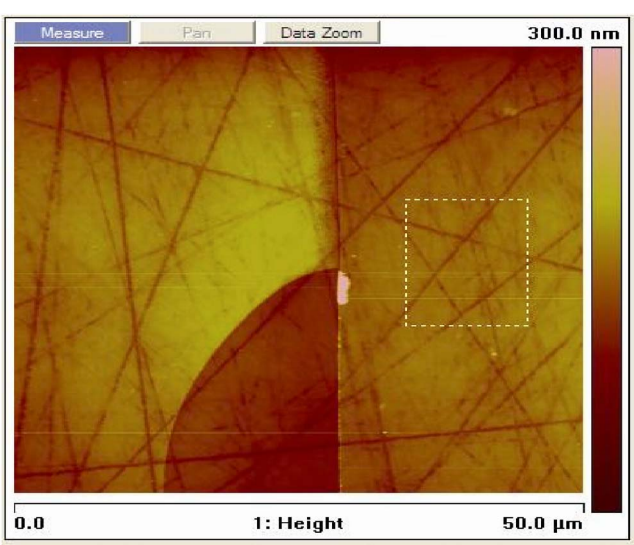

FIG. 6. (Color online) An AFM scan of the surface of one of our samples. For the region within the dotted rectangle, the average roughness is 6 nm. The maximum height of any feature in the dotted rectangle is 69 nm.

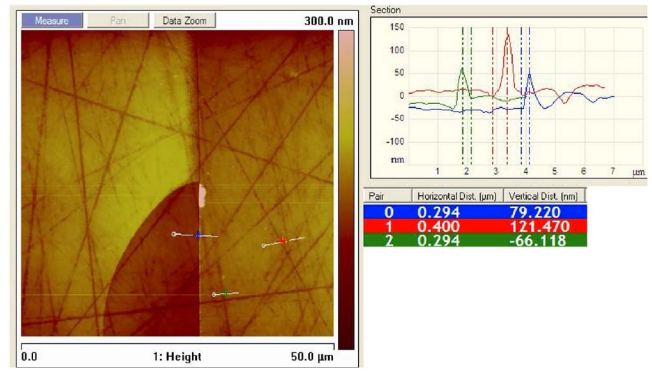

FIG. 7. (Color online) Line scans over three visible protrusions on the AFM image. For each scan we measure the height and base length of the protrusion using the upper right plot. The numbers for each scan appear in different color lines below the figures.

All visible protrusions appear to have $c/b<1$. If there are any features with the appropriate c/b ratio, their base dimensions are so small that they are not individually discernible. Referring back to Fig. 7, we see that the aggregate of all such protrusions would have a maximum height of 70 nm. That would mean that the only possible agreement with the theory can be for the data of 0.8 μm separation. In all other cases, the predictions of the theory are either unrealistic $[A>(80\ \mu\text{m})^2]$ or the required dimensions of the protrusion responsible for the field amplification are outside the range of those found with the AFM scans. This is the second piece of evidence that the theory cannot explain our data.

V. DISCUSSION

The analysis done for data in the regime where electrical breakdown is thought to be the result of field emission of electrodes assumes a field amplification factor on the surface of the electrodes. Any calculations made (e.g., Refs. 18 and 19) regarding the height or surface area of a surface feature responsible for such an amplification assumes that the current observed is due to emission from a single protrusion. We have tested that assumption by calculating the amount of current, as a function of applied voltage, that would be produced by a variety of protrusions of different aspect ratios and shapes. The choice of shape does not appear to change our conclusions significantly. Here, the shape of the features was chosen to be a hemisphere on top with vertical sides, to control the aspect ratio, that end on hemispheres with the opposite curvature to connect to a flat surface (as shown in the inset of Fig. 8). The results of our calculations are presented in Fig. 8.

We have plotted $\ln(I/V^2)$ vs $1/V$, since this is clearly the form of the data that is more crucial to the analysis. The current is the total current emitted by the protrusion due to the enhanced field at each point on the protrusion. The results represent currents induced from protrusion of aspect ratios of 2, 4, 8, 10, and 20. It is evident from this figure that the differences in aspect ratios of an order of magnitude would produce currents that would differ by a factor of ~150 [a difference of less than 6 in the $\ln(I/V^2)$ vs $1/V$ plot]. That is, there is no reason to assume that a single protrusion dominates the current emission, especially when

Downloaded 29 Dec 2006 to 129.6.64.224. Redistribution subject to AIP license or copyright, see http://jap.aip.org/jap/copyright.jsp

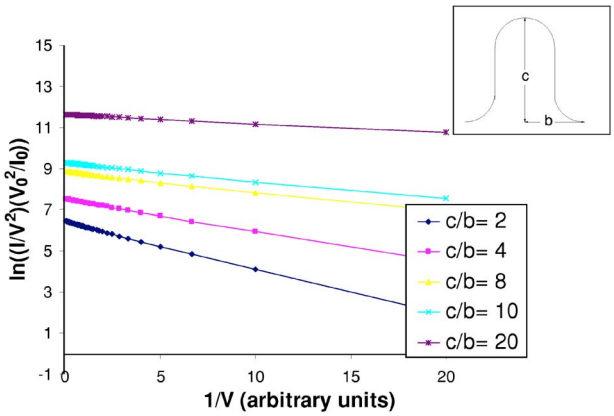

FIG. 8. (Color online) Simulations of $\ln[I/V^2(V_0^2/I_0)]$ vs $1/V$ for protrusion of different aspect ratios.

doing an analysis based on $\ln(1/V^2)$. In our opinion this means that a collection of noninteracting protrusions of different aspect ratios can produce a current that would appear to be caused by a single protrusion of larger aspect ratio.

The calculation of the emitting area A then would only be the sum of the areas of all the different protrusions involved in the measured current. In such a case, the calculations of the height for a single protrusion based on its base dimension, for physical values of calculated A as done in Table I, are not necessarily correct. For these cases the features responsible for the observed current may be a collection of smaller features, in height and base dimension, even of different aspect ratios between them.

The standard theory is not helpful in predicting the characteristics of such features. Although the above assumption of a large number of noninteracting protrusions provides a possible explanation as to why the standard theory breaks down in the case of analyzing our data, it does not explain why in some cases the calculated emitting area is much larger than the actual size of our electrodes. Also, having measured no visible protrusion of aspect ratio more than 1, to our AFM precision, and knowing that evaporated Au makes rather smooth films (typical size of features is 20–30 nm in diameter, but only ~5 nm tall[21]), it seems rather unlikely that there would be features of much smaller base dimensions and similar aspect ratios to those calculated. The reasoning above leads us to the conclusion that even in the case of the 0.8 μm of electrode separation it is unlikely that the data agree with the theory. In that case the theory predicts values for the emitting area that are smaller than the precision of the AFM measurement, but also predicts an aspect ratio of ~20 for the surface features, that seems quite improbable given the typical surface characteristics of evaporated Au.

Finally, some of the reasons for the enhanced local electric field on the surface of electrodes, mentioned in studies such as Refs. 9–15, do not seem to apply in our case. For example, it is suggested that gas molecule desorption or foreign element contamination of the electrodes would locally enhance the electric field. These reasons refer to bulk metal electrodes and should not be possible in our thin film evaporated electrodes. Also, our measurements are done in atmospheric air and so the electrodes do not have any contact with any other gases.

VI. SUMMARY

We have presented data for breakdown of air for electrode separations between 400 nm and 45 μm. For the data below 10 μm, it appears that the mechanism responsible for the breakdown is field emission of electrons, based on the good agreement between the theory and our $\ln(I/V^2)$ vs $1/V$ plots. This is the same mechanism that governs breakdown in vacuum. Using the standard Fowler-Nordheim equations for field emission we see that a field magnification factor is needed to explain the data. The standard theory claims that protrusions of a certain geometry on the surface of the conductors are responsible for such field amplification factors. We have used the standard theory to calculate the dimensions of such protrusions.

Using an AFM we have looked for such features on the surface of our electrodes. We have found three pieces of evidence that the theory does not apply to our data. First, some of the calculated values of areas of surface features exceed the dimensions of our electrodes. Second, no protrusions with the correct height to base ratio exist on our electrodes that could explain our data (except, perhaps, for the data of 0.8 μm of separation). Third, the fact that we used evaporated Au seems to exclude the possibility of features of the correct aspect ratios that are smaller than our resolution. We have also shown that in some cases the assumption made by the theory that a single feature is responsible for the observed current is not valid.

We therefore must conclude that a different theory is needed for explaining the field amplification and field emission of electrons in our data.

ACKNOWLEDGMENTS

The authors would like to thank Dr. Richard Gates for his help with the AFM measurements, and Dr. Lee Richter, Dr. James Olthoff, and Brian Simonds for their help in understanding the bibliography and for useful discussions.

[1]M. J. Madou, *Fundamentals of Microfabrication: The Science of Miniaturization* (CRC, Boca Raton, FL, 2002).
[2]H. R. Shea A. Gasparyan, H. B. Chan, S. Arney, R. E. Frahm, D. Lopez, S. Jin, and R. P. McConnell, IEEE Trans. Device Mater. Reliab. **4**, 198 (2004).
[3]J. Dillon, *Gaseous Conductors: Theory and Engineering Applications* (Dover, New York, 1958).
[4]P. G. Slade and E. D. Taylor, IEEE Trans. Compon. Packag. Technol. **25**, 390 (2002).
[5]A. Wallash and L. Levit, Proc. SPIE **4980**, 87 (2003).
[6]D. K. Davies and M. A. Biondi, J. Appl. Phys. **37**, 2969 (1966).
[7]I. Brodie, J. Appl. Phys. **35**, 2324 (1964).
[8]W. S. Boyle, P. Kisliuk, and L. H. Germer, J. Appl. Phys. **26**, 720 (1955).
[9]A. Jankowiak, P. Fourcade, and R. Blanchart, J. Eur. Ceram. Soc. **25**, 2821 (2005).
[10]G. Sotgiu and L. Schirone, Appl. Surf. Sci. **240**, 424 (2005).
[11]D. Nicolaescu *et al.*, J. Vac. Sci. Technol. B **22**, 1227 (2004).
[12]T. Wang, C. E. Reece, and R. M. Sundelin, J. Vac. Sci. Technol. B **21**, 1230 (2003).
[13]T. Wang, C. E. Reece, and R. M. Sundelin, Rev. Sci. Instrum. **73** 3215 (2002).
[14]A. A. Neuber *et al.*, IEEE Trans. Plasma Sci. **28**, 1593 (2000).

Downloaded 29 Dec 2006 to 129.6.64.224. Redistribution subject to AIP license or copyright, see http://jap.aip.org/jap/copyright.jsp

[15]A. Neuber *et al.*, J. Appl. Phys. **85**, 3084 (1999).
[16]R. Gomer, *Field Emission and Field Ionization* (Harvard University Press, Cambridge, MA, 1961).
[17]A. Modinos, *Field, Thermionic, and Secondary Electron Emission Spectroscopy* (Plenum, New York, 1984), p. 16.
[18]F. M. Charbonnier and E. E. Martin, J. Appl. Phys. **33**, 1897 (1962).
[19]G. T. Boyd, Th. Rasing, J. R. R. Leite, and Y. R. Shen, Phys. Rev. B **30**, 519 (1984).
[20]E. Hourdakis, B. J. Simonds, and N. M. Zimmerman, Rev. Sci. Instrum. **77**, 034702 (2006).
[21]D. Porath, O. Millo, and J. I. Gersten, J. Vac. Sci. Technol. B **14**, 30 (1996).

Downloaded 29 Dec 2006 to 129.6.64.224. Redistribution subject to AIP license or copyright, see http://jap.aip.org/jap/copyright.jsp